Tunneling chemical reactions in solid parahydrogen: Direct measurement of the rate constants of R+H-2 -> RH+H (R=CD3,CD2H,CDH2,CH3) at 5 K

AUTHOR(S):

Hoshina, H; Fushitani, M; Momose, T; Shida, T

CITATION:

Hoshina, H ...[et al]. Tunneling chemical reactions in solid parahydrogen: Direct measurement of the rate constants of R+H-2 -> RH+H (R=CD3,CD2H,CDH2,CH3) at 5 K. JOURNAL OF CHEMICAL PHYSICS 2004, 120(8): 3706-3715

ISSUE DATE:

2004-02-22

URL:

http://hdl.handle.net/2433/50047

JOURNAL OF CHEMICAL PHYSICS VOLUME 120, NUMBER 8 22 FEBRUARY 2004

Tunneling chemical reactions in solid parahydrogen: Direct measurement of the rate constants of $R+H_2 \rightarrow RH+H$ ($R=CD_3, CD_2H, CDH_2, CH_3$) at 5 K

Hiromichi Hoshina, Mizuho Fushitani,[a] and Takamasa Momose
Division of Chemistry, Graduate School of Science, Kyoto University, Kyoto 606-8502, Japan

Tadamasa Shida
Kanagawa Institute of Technology, Atsugi 243-0292, Japan

(Received 5 June 2003; accepted 25 November 2003)

Tunneling chemical reactions between deuterated methyl radicals and the hydrogen molecule in a parahydrogen crystal have been studied by Fourier transform infrared spectroscopy. The tunneling rates of the reactions $R+H_2 \rightarrow RH+H$ ($R=CD_3, CD_2H, CDH_2$) in the vibrational ground state were determined directly from the temporal change in the intensity of the rovibrational absorption bands of the reactants and products in each reaction in solid parahydrogen observed at 5 K. The tunneling rate of each reaction was found to differ definitely depending upon the degree of deuteration in the methyl radicals. The tunneling rates were determined to be 3.3×10^{-6} s^{-1}, 2.0×10^{-6} s^{-1}, and 1.0×10^{-6} s^{-1} for the systems of CD_3, CD_2H, and CDH_2, respectively. Conversely, the tunneling reaction between a CH_3 radical and the hydrogen molecule did not proceed within a week's time. The upper limit of the tunneling rate of the reaction of the CH_3 radical was estimated to be 8×10^{-8} s^{-1}. © *2004 American Institute of Physics.* [DOI: 10.1063/1.1642582]

I. INTRODUCTION

The tunneling effect becomes important in chemical reactions at low temperature because of the suppression of thermally activated reaction processes. Such a situation is expected to be realized in interstellar clouds, for example.[1] However, the determination of bimolecular rate constants for cryogenic reactions is not easy because most systems are immobilized by condensation at low temperatures.

Compared with this difficulty inherent in bimolecular reactions, unimolecular reactions involving intramolecular tunneling processes are relatively easy to study in cryogenic crystals. For example, a long-range hydrogen transfer by tunneling in a radiation damaged dimethylglyoxime crystal was studied by electron spin resonance (ESR) spectroscopy.[2] Hydrogen atom exchange by tunneling in a malonaldehyde crystal was also studied using microwave spectroscopy.[3] More recently, a *cis–trans* isomerization of formic acid in rare gas matrices was studied in connection with the matrix effect on the tunneling process in the isomerization.[4]

As for bimolecular reactions, the reaction $CH_3+CH_3OH \rightarrow CH_4+CH_2OH$ was studied extensively using ESR spectroscopy.[5,6] Another example of the bimolecular reaction by tunneling was reported between hydrogen atoms and molecules.[7,8] We ourselves have been studying the reaction between methyl radicals and the parahydrogen molecule in a parahydrogen crystal (p-H_2) at cryogenic temperatures.[9,10]

In the present work we extend our previous studies by covering all isotopomeric radicals CD_3, CD_2H, CDH_2, and CH_3. The aim of the present study is to shed more light on the intrinsic nature of the reactions promoted by tunneling. In order to provide a general background to our study, we will first recapitulate our previous work.

During the past decade we have been studying rovibrational spectra of molecules embedded in solid p-H_2 which has several salient features in both high resolution spectroscopic and *in-situ* photolytic studies.[9–23] The p-H_2 matrix is capable of providing not only high resolution spectroscopic information regarding embedded molecules but also subtle intermolecular interaction between trapped molecules and the matrix hydrogen molecule.[12,13,15–18,21,22] The feasibility of the study of *in-situ* photolysis stems from the fact that molecules in solid p-H_2 happen to be free from the cage effect, which allows us to study photolytically produced fragments such as radicals originating from the parent molecule.[9,14,23–26]

In a previous paper we have observed Fourier transform infrared (FTIR) spectra of the CD_3 radical trapped in solid p-H_2 crystal.[9] The decrease in the absorption intensity of CD_3 and the increase in the intensity of CD_3H were observed over a span of about one week at 5 K. As a result of that study, it was found that CD_3 reacts with surrounding hydrogen molecules through tunneling as follows:

$$CD_3+H_2 \rightarrow CD_3H+H.$$

Since the activation energy of the above reaction has been estimated to be 11–14 kcal/mol ($\simeq$5500–7000 K),[27,28] the occurrence of the above reaction at 5 K must be ascribed exclusively to pure tunneling. Assuming that the reaction can

[a]Present address: Institut fuer Experimentalphysik, Fachbereich Physik, Freie Universitaet Berlin, Arnimallee 14, D-14195 Berlin, Germany.

be expressed by a pseudo first-order rate law, the tunneling rate constant was determined to be $(4.7\pm0.5)\times10^{-6}$ s^{-1}.[9] In the same experiment no appreciable spectral change was observed for the $CH_3/p\text{-}H_2$ system under the same conditions. This difference between the two systems was explained in terms of the enthalpic difference including the zero-point energies of the reactants and products. The reaction between the methyl radical and hydrogen molecule is nearly thermoneutral since the zero-point dissociation energies of H_2 ($D_0=4.4781$ eV)[29] and CH_4 ($D_0=4.406$ eV)[30] are very close. Consequently, the small difference in zero-point vibrational energies between the $CD_3/p\text{-}H_2$ and $CH_3/p\text{-}H_2$ reaction systems would cause the drastic change in the tunneling rate.

In the present work we have improved the spectroscopic resolution from 0.25 cm^{-1} for the previous work to 0.1–0.01 cm^{-1} and compared all the four isotopomeric systems. As a result, a systematic difference in the rate constant of the tunneling reaction was revealed. In order to find further clues for the quantum level dependence of the tunneling reaction, a preliminary test on the effect of the monitoring IR beam on the reaction rate was also attempted.

II. EXPERIMENT

Solid parahydrogen used as the matrix was prepared by the same technique described in our previous papers.[9,25] The methyl radicals, CH_3, CDH_2, CD_2H, and CD_3, were produced through *in-situ* photolysis of the corresponding methyl iodides CH_3I, CDH_2I (>98 atom %D), CD_2HI (>98 atom %D), and CD_3I (>99 atom %D), which were premixed with the $p\text{-}H_2$ gas containing less than 0.05% of orthohydrogen.[10] The admixture was introduced into a copper optical cell kept at about 8.2 K to grow a transparent mixed crystal. The size of the optical cell was 3.0 cm in length and 1.7 cm in diameter. BaF_2 was used for the windows of the optical cell and the cryostat. A low pressure 20 W Hg lamp emitting both 253.7 nm and 184.9 nm photons was employed for photolysis of the iodides. A 4-hour long UV irradiation gave sufficient concentrations of the methyl radicals.

A Bruker IFS 120HR FTIR spectrometer was used throughout the experiment. To cover both the mid-IR and near-IR spectral regions two types of the light sources were employed: for the mid-IR region (10–2 μm) a glowbar source was used, while for the near-IR region (2–1 μm) a tungsten lamp was used. A KBr beam splitter and a liquid nitrogen cooled HgCdTe (MCT) detector were used in common to the measurements of the two spectral regions.

After the UV irradiation, the following three different measurements were performed in order to examine any possible effect of the light source on the samples:

(1) The IR spectra were measured with no optical filter between the light sources and the sample. Since the sample was exposed for a long period to the monitoring IR beam covering a range of 700 cm^{-1}, which was a limit of transmission of the BaF_2 windows, through 7500 cm^{-1}, a limit of the KBr beam splitter, it was suspected that the light sources might have some effect on the sample in this mode of measurement. The results of the measurement are listed in the second row of Tables II and III.

(2) To test the suspicion mentioned in the measurement (1) above, spectral recording was carried out with several IR filters inserted between the light sources and the sample. Depending upon the spectral bands of our interest, several filters were selected as summarized in the third, fourth, and fifth rows of Tables II and III. To be more specific, IR filters passing either ranges of 785–1390 cm^{-1} or 2170–3905 cm^{-1} were used for CD_3I, a filter of 2170–3905 cm^{-1} for CD_2HI, and a filter of 1330–2240 cm^{-1} for CDH_2I, respectively.

(3) To further test the possible effect of exposing the sample to the monitoring beam, the measurement 3 was also made, where the light sources were turned off except for the period of spectral scanning which took about 1 or 2 hours for both the mid-IR (with a glowbar source) and the near-IR (with a tungsten lamp). During the remaining 22 to 23 hours of the day, the sample was kept in complete darkness. This measurement regime was repeated every day for about one week. Since the effect of this turning off the light sources turned out to be negligible, the measurement (3) was made only for the $CD_3I/p\text{-}H_2$ system as shown in the last row of Tables II and III.

The temperature of the crystal was maintained at 5 $\pm$0.1 K throughout the duration of the experiment.

III. RESULTS AND DISCUSSION

A. Observed spectra

Figures 1–4 show the results of the systems of $CD_3I/p\text{-}H_2$, $CD_2HI/p\text{-}H_2$, $CDH_2I/p\text{-}H_2$, and $CH_3I/p\text{-}H_2$ recorded using the measurement (1) stated in Sec. II.

In these figures trace (I) shows spectra as deposited at 5 K, trace (II) after a four-hour UV irradiation, and trace (III) the same as trace (II) after one week. In each figure spectra due to methane ($CD_3H, CD_2H_2, CDH_3, CH_4$) are shown at the bottom for the convenience of comparison with the spectra of products seen in (II) and (III). The symbols I, R, and M stand for methyl iodide, methyl radical, and methane, respectively. The observed frequencies of the vibrational fundamental bands of the iodides, the radicals, and the methanes are summarized in Table I along with the values observed in the gas phase[31,32] or the values obtained by an *ab-initio* calculation.[33] In the table, frequencies at the center of the band are adopted as the frequency of the band origin in solid $p\text{-}H_2$. The details of the results of each system is discussed below.

1. CD_3I

Trace (I) of Fig. 1 shows the ν_2 and ν_4 fundamental bands of CD_3I peaking at 947 and 2298 cm^{-1}. These are close to the reference values in the gas phase.[31] Trace (II) shows the spectra due to the perdeuterated methyl radical (R) and the residual iodide,

$$CD_3I \xrightarrow{253.7\ \text{nm}+184.9\ \text{nm}} CD_3+I. \quad (1)$$

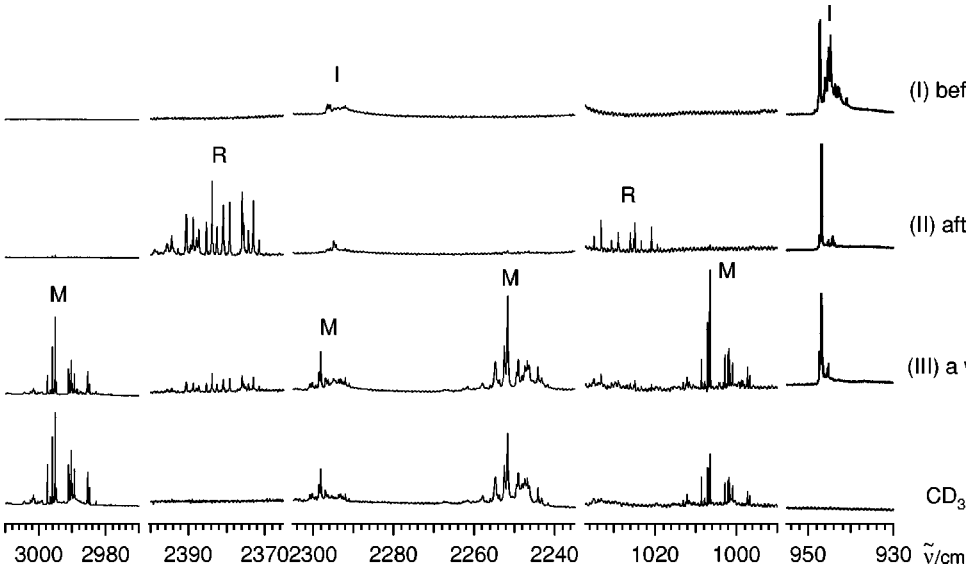

FIG. 1. Infrared absorption spectra of CD_3I in solid p-H_2. (I) As deposited at 5 K. (II) Same as (I) after a 240 min UV irradiation. (III) Same as (II) after one week. The spectra at the bottom is CD_3H in solid p-H_2 at 4.8 K. The symbols, I, R, and M stand for the methyl iodide (CD_3I), methyl radical (CD_3), and methane (CD_3H), respectively. Spectra (I)–(III) are displayed in the same scale.

The ν_3 and ν_4 bands of CD_3 were observed at 2379 cm^{-1} and 1034 cm^{-1} respectively. Contrary to the previous paper where the ν_3 band of CD_3 was heavily overlapped with the absorption band of CO_2, the spectrum in trace (II) of Fig. 1 shows an uncontaminated ν_3 band of CD_3 because the residual air in the spectrometer was evacuated in the present experiment. Structures of the ν_3 and ν_4 bands are attributed to the molecular rotation and to the crystal field splitting as in the case of the previous work.[12,34]

Although almost unrecognizable in trace (II) of Fig. 1, a very weak absorption due to CD_2H_2 was observed at 2973 cm^{-1}. This methane was produced via the following reactions[25] (cf. bottom of Fig. 2):

$$\begin{aligned} &CD_3 \xrightarrow{184.9\ \text{nm}} CD_2 + D, \\ &CD_2 + H_2 \rightarrow CD_2H_2. \end{aligned} \tag{2}$$

Trace (III) of Fig. 1 recorded after one week demonstrates sharp peaks at 2990, 2248, 1035, and 1002 cm^{-1}, all of them being attributable to CD_3H as is supported by the nice matching with the authentic spectrum shown at the bottom of Fig. 1.

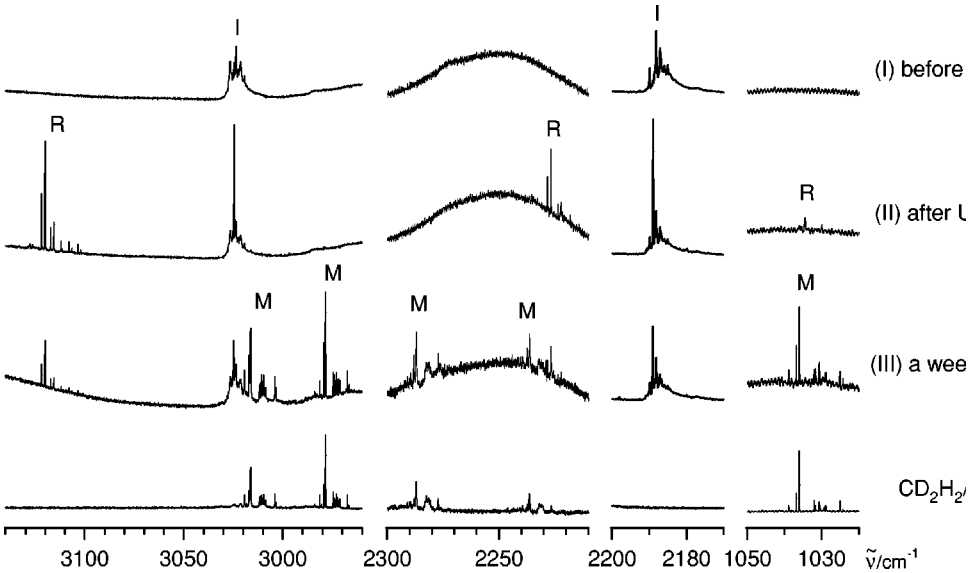

FIG. 2. Infrared absorption spectra of CD_2HI in solid p-H_2. (I) As deposited at 5 K. (II) Same as (I) after a 240 min UV irradiation. (III) Same as (II) after one week. The spectra at the bottom is CD_2H_2 in solid p-H_2 at 4.8 K. The symbols, I, R, and M stand for the methyl iodide (CD_2HI), methyl radical (CD_2H), and methane (CD_2H_2), respectively. Spectra (I)–(III) are displayed in the same scale.

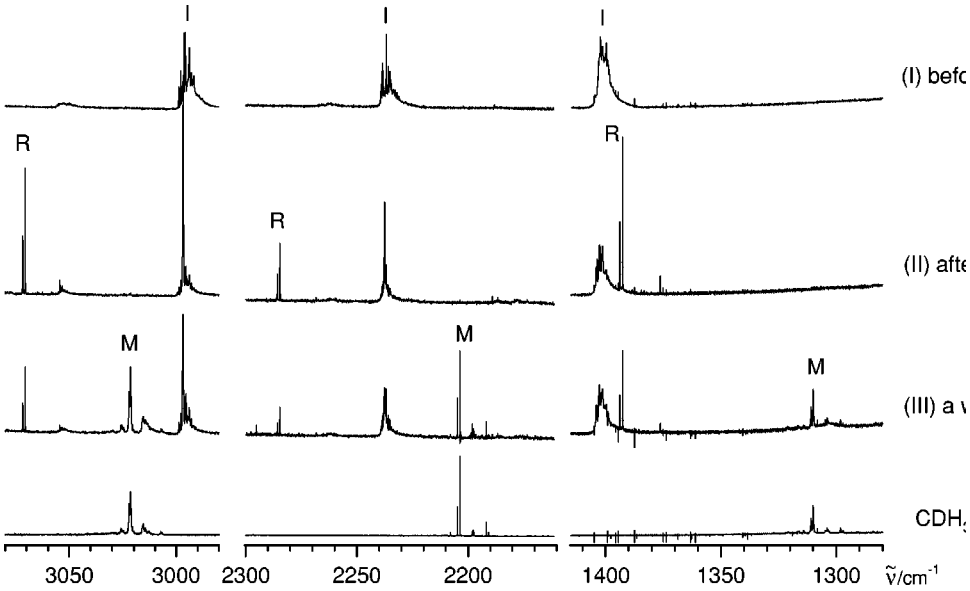

FIG. 3. Infrared absorption spectra of CDH_2I in solid p-H_2. (I) As deposited at 5 K. (II) Same as (I) after a 240 min UV irradiation. (III) Same as (II) after one week. The spectra at the bottom is CDH_3 in solid p-H_2 at 4.8 K. The symbols, I, R, and M stand for the methyl iodide (CDH_2I), methyl radical (CDH_2), and methane (CDH_3), respectively. Spectra (I)–(III) are displayed in the same scale.

2. CD_2HI

The 3027 cm^{-1} band in trace (I) of Fig. 2 assigned to the ν_4 absorption of CD_2HI/p-H_2 is in good agreement with the gas phase spectrum.[32] The absorption bands around 3121, 2228, and 1035 cm^{-1} in trace (II) are close to those of the CD_2H radical observed in the gas phase. They also compare favorably with the results of the *ab initio* calculation for the radical[33] and can be assigned to the ν_1, ν_5, and ν_3 bands of CD_2H, respectively. Comparison of trace (III) with the spectrum at the bottom of Fig. 2 clearly indicates that the peaks at about 3010, 2973, 2265, 2231, and 1031 cm^{-1} are associated with ν_6, ν_1, $\nu_4+\nu_9$, ν_8, and ν_4 of CD_2H_2, respectively.

3. CDH_2I

In trace (I) of Fig. 3 the ν_4, ν_1, and ν_5 bands of CDH_2I are observed at 2997, 2237, and 1402 cm^{-1} which are close to those in the gas phase.[32] The bands at around 3071, 2285, and 1393 cm^{-1} in trace (II) can be assigned to the ν_5, ν_2,

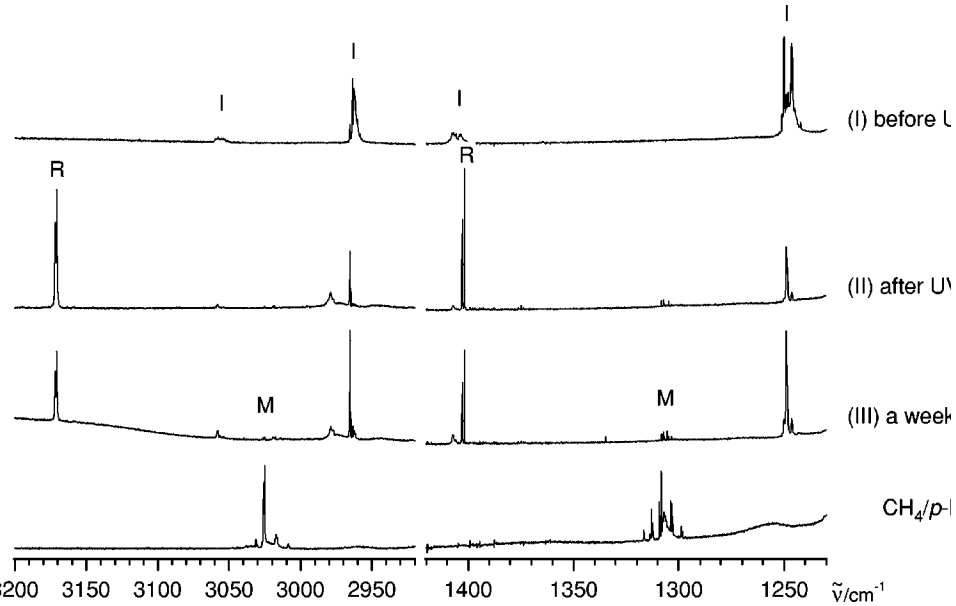

FIG. 4. Infrared absorption spectra of CH_3I in solid p-H_2. (I) As deposited at 5 K. (II) Same as (I) after 240 min UV irradiation. (III) Same as (II) after one week. The spectra at the bottom is CH_4 in solid p-H_2 at 4.8 K. The symbols, I, R, and M stand for the methyl iodide (CH_3I), methyl radical (CH_3), and methane (CH_4), respectively. Spectra (I)–(III) are displayed in the same scale.

TABLE I. The observed and calculated wave numbers of the vibrational absorption bands of deuterated methyl iodides, methyl radicals, and methanes in solid p-H_2. The units are in cm^{-1}. Labels in the parentheses represent the character of the vibrational modes.

	CH_3I		CD_3I			CDH_2I		CD_2HI	
(C_{3v})	p-H_2	gas[a]	p-H_2	gas[a]	(C_s)	p-H_2	gas[b]	p-H_2	gas[b]
ν_1 (a_1)	2979	2970	2151	2155	ν_1 (a')	2237	2241	2189	2194
ν_2 (a_1)	1249	1252	947	951	ν_2 (a')	1171	1172	1016	1018
ν_3 (a_1)		533		501	ν_3 (a')		518		508
ν_4 (e)	3059	3060	2298	2298	ν_4 (a')	2997	3002	3027	3030
ν_5 (e)	1433	1436	1047	1049	ν_5 (a')	1402	1415	1170	1170
ν_6 (e)	886	882		656	ν_6 (a')		710		754
					ν_7 (a'')	3055	3057	2341	2336
					ν_8 (a'')	1234	1240	1280	1287
					ν_9 (a'')	866	862		659

	CH_3			CD_3			CDH_2		CD_2H	
(D_{3h})	p-H_2	gas[a]	calc.[c]	p-H_2	gas[a]	calc.[c]	(C_{2v})	p-H_2	calc.[c]	p-H_2	calc.[c]
ν_1 (a_1')		3004	2925		2158	2070	ν_1 (a_1)		2985	3121	3035
ν_2 (a_2'')		606	620		458	460	ν_2 (a_1)	2285	2210		2135
ν_3 (e')	3171	3161	3080	2379	2381	2300	ν_3 (a_1)	1393	1365	1035	1015
ν_4 (e')	1402	(1396)[d]	1370	1034	(1029)[d]	1015	ν_4 (b_1)		570		520
							ν_5 (b_2)	3071	3080	2228	2295
							ν_6 (b_2)	1179	1145	1281	1255

	CH_4			CD_3H		CDH_3			CD_2H_2	
(T_d)	p-H_2	gas[a]	(C_{3v})	p-H_2	gas[a]	p-H_2	gas[a]	(C_{2v})	p-H_2	gas[a]
ν_1 (a_1)		2917	ν_1 (a_1)	2990	2993	2972	2973	ν_1 (a_1)	2973	2976
ν_2 (e)		1534	ν_2 (a_1)	2140	2142	2198	2200	ν_2 (a_1)		2202
ν_3 (f_2)	3017.3	3019	ν_3 (a_1)	1002	1003	1304	1300	ν_3 (a_1)		1436
ν_4 (f_2)	1303.6	1306	ν_4 (e)	2248	2263	3015	3017	ν_4 (a_1)	1031	1033
			ν_5 (e)	1290	1291	1472	1471	ν_5 (a_2)		1329
			ν_6 (e)	1035	1036	1155	1155	ν_6 (b_1)	3010	3013
								ν_7 (b_1)	1090	1090
								ν_8 (b_2)	2231	2234
								ν_9 (b_2)	1234	1234

[a]Reference 31.
[b]Reference 32.
[c]Reference 33.
[d]Ne matrix measurement.

and ν_3 bands of the CDH_2 radical, respectively, from the comparison with the calculation.[33] Reference to the spectrum at the bottom of Fig. 3 supports the assignment of the bands at about 3015, 2198, and 1304 cm^{-1} in trace (III) to the ν_4, ν_2, and ν_3 bands of CDH_3, respectively.

4. CH_3

Figure 4 for the prototypical system is shown for the sake of the completeness of all the isotopomeric systems. The result in Fig. 4 is in complete agreement with the result of our previous work.[9,25] In brief, the conversion from the CH_3 radical (R) to methane (M) was almost negligible during the one week standing [cf. (II) and (III) in Fig. 4]. The decrease in the intensity of R was counterbalanced by the increase in the intensity of the methyl iodide (I). This result suggests that only some of the radicals recombined with the geminately produced iodine atom. Details of the recombination are also discussed below.

B. Spectral change

A common feature throughout Figs. 1–3 is that the absorption of the radicals observed in trace (II) diminished, to be replaced by the absorption of the appropriate methane, shown in trace (III). From this result the following reaction scheme is immediately derived in accordance with our previous study:[9]

$$\mathrm{R}+\mathrm{H_2}\xrightarrow{k}\mathrm{RH}+\mathrm{H}$$
$$(\mathrm{R}=\mathrm{CD_3},\ \mathrm{CD_2H},\ \mathrm{CDH_2}). \tag{3}$$

In sharp contrast to Figs. 1–3, the pure isotope system shown in Fig. 4 showed almost no measurable change in one week. This result indicates that the tunneling reaction between CH_3 radical and parahydrogen does not occur or is too slow to detect by our experiment,

$$\mathrm{CH_3}+\mathrm{H_2}\not\rightarrow\mathrm{CH_4}+\mathrm{H}. \tag{4}$$

Figures 5 and 6 demonstrate the temporal change in the intensity of the absorption band of various methyl radicals

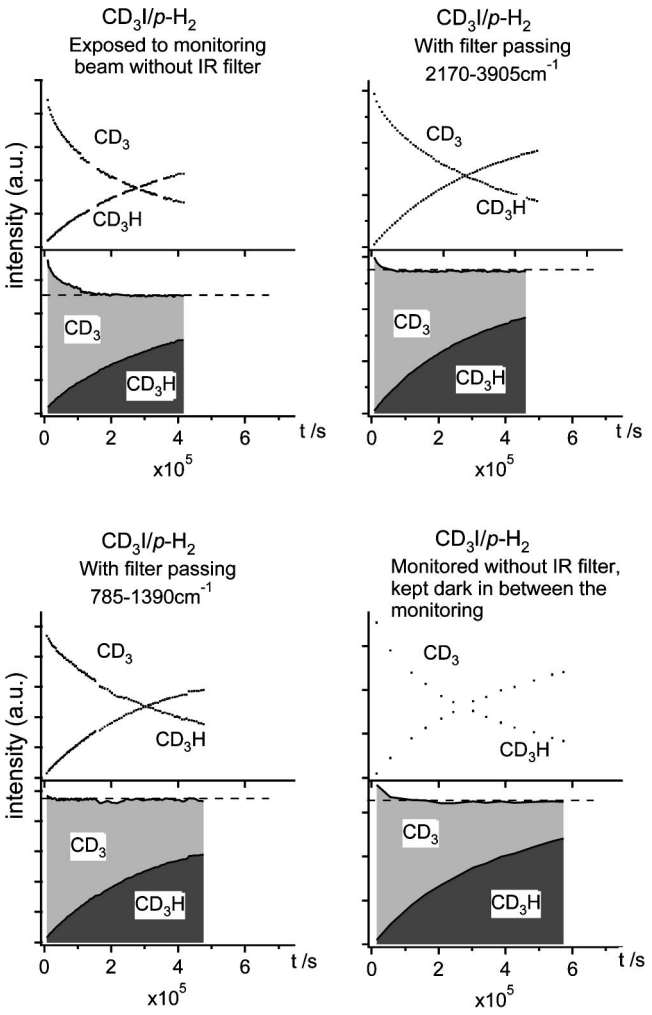

FIG. 5. The temporal change of CD_3 and CD_3H in solid p-H_2 at 5 K after UV irradiation. Upper left, the sample was exposed to the monitoring IR beam throughout the experiment with no IR filter being inserted. Lower left, same as above with a filter passing 785–1390 cm^{-1}. Upper right, same as the lower left except that a filter passing 2170–3905 cm^{-1} was used. Lower right, same as the upper left, but during the idle period of the optical measurement the light source was turned off.

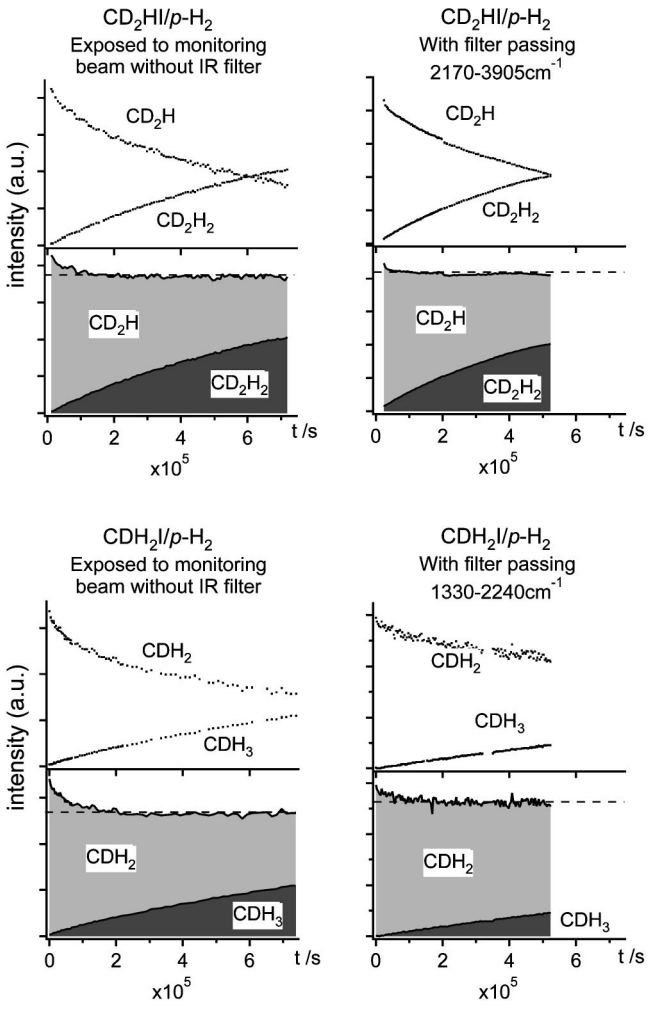

FIG. 6. The temporal changes of CD_2H and CD_2H_2 (the upper two panels) and the changes of CDH_2 and CDH_3 (the lower two panels). Upper left, the sample was exposed to the monitoring IR beam throughout the experiment with no filters being inserted. Upper right, same as the left except that a filter passing 2170–3905 cm^{-1} was used. Lower left, the sample was exposed to the monitoring IR beam throughout the experiment with no IR filters being inserted. Lower right, same as the left except that a filter passing 1330–2240 cm^{-1} was used.

and the corresponding methanes produced by the irradiation of CD_3I, CD_2HI, and CDH_2I systems. The changes obtained using different filters or the masurement (3) stated in Sec. II are compared in Figs. 5 and 6 for later discussion. Probably because the baseline determination was not very reliable owing to the long-term fluctuation of the background signal, the absorption intensities obtained by the direct integration of the observed band turned out to deviate quite significantly. In order to reduce the deviation, the absorption intensity was obtained by assuming a Lorentzian line shape to which the recorded spectral bands were least-squares fitted. In each panel the upper half shows the temporal changes of the methyl radicals and the counterpart methanes in arbitrary units, the latter change being multiplied by an arbitrary constant so as to make the decay of the radicals and the increase of the methanes look as if they were mirror images.

In order to interpret the results shown in the upper part of each panel of Figs. 5 and 6 we have attempted the following two analyses. Eventually, the second method of analysis was adopted for later discussion. However, the result of both methods is explained herein. In the first analysis it was assumed that the temporal changes of the radicals and the methanes were entirely due to the reactions in Eq. (3). In this case the sum of the numbers of disappearing radicals and appearing methanes should remain constant as expressed in Eq. (5), where I_R and I_M represent the integrated intensities and A_R and A_M stand for the absorption coefficients of the radicals and methanes, respectively,

$$\frac{I_R}{A_R}+\frac{I_M}{A_M}=\text{const.} \tag{5}$$

The unknown parameters A_R and A_M were determined by least-squares fitting. The result of the fittings, however, totally disproved the constancy of the above equation over the entire time of all observations.

As a succeeding trial, it was presumed that some of the radicals were formed and decayed independently of the counterbalancing reaction (3). This presumption is based on

TABLE II. First-order rate constants for the rapidly decaying component of the CD_3, CD_2H, and CDH_2 radicals. The numbers in the table represent the first-order rate constant (k) in units of 10^{-6} s^{-1}. The decay corresponds to the area shown in gray exceeding the broken horizontal lines in Fig. 5. Because the temporal change of this component was rapid and weak the precision of the rate constants in Table II is inferior to that in Table III. The second through sixth rows correspond to the three sets of conditions used in the experiments (see text in Sec. II).

	CD_3	CD_2H	CDH_2
No IR filter	18±11	16±20	15±12
Filter (2170–3905 cm^{-1})	49±26	21±41	
Filter (1330–2240 cm^{-1})			17±57
Filter (785–1390 cm^{-1})	66±25		
Dark	30±21		

the graphical features seen in the lower part of each panel which show the summation of the intensities of the methanes in black area and the radicals in gray. It is seen that the level of the summation becomes quickly horizontal (within less than 2×10^5 s) as shown in broken lines and that in the early stage a rapidly decaying component of the radical exists. It was found that the rapidly decaying component roughly fits an exponential curve, for which the exponents are summarized in Table II. The variance of the exponents is admittedly large. All we can say is that a small fraction of the methyl radicals is subjected to a fast decay process, perhaps a recombination with the counterpart iodine atom produced from the parent iodide through photolysis.

The fact that a horizontal line is attained by subtracting the above rapidly decaying component suggests that the major component of the radical is associated with the reaction (3), which requires that the sum of the radical and the methane produced therefrom remains constant over the entire time of all observations. In the next section this major reaction (3) will be discussed after the examination of the geminate recombination between the radical and the iodine atom.

C. Reaction rate

1. Recombination between methyl radical and iodine atom

In order to substantiate the assumption of the additional reaction of the radical with the counterpart iodine atom we have surveyed the near infrared region of the photolyzed sample. In that region the magnetic dipole allowed transition of the iodine atom, $^2P_{1/2}\leftarrow{}^2P_{3/2}$, is known to exhibit a characteristic peak at 7638 cm^{-1}.[26] The peak was detected easily and showed a temporal change, as illustrated for the CD_3I system in the upper panel of Fig. 7. Concomitantly, one of the absorption lines of CD_3I observed at 947.3 cm^{-1} increased as shown in the lower panel of Fig. 7. The rates of the decay and the increase was found to be in agreement with each other within their standard deviations. Similar comparative measurements were done for all the iodide systems with no IR filter being set in between the sample and the monitoring IR beam. The observed decay rate of the iodine atom $1.0–1.1\times10^{-5}$ s^{-1} was found to be comparable with the rate of the rapid decay of the radicals as listed in Table II. These results suggest that some of the photolyzed iodides left

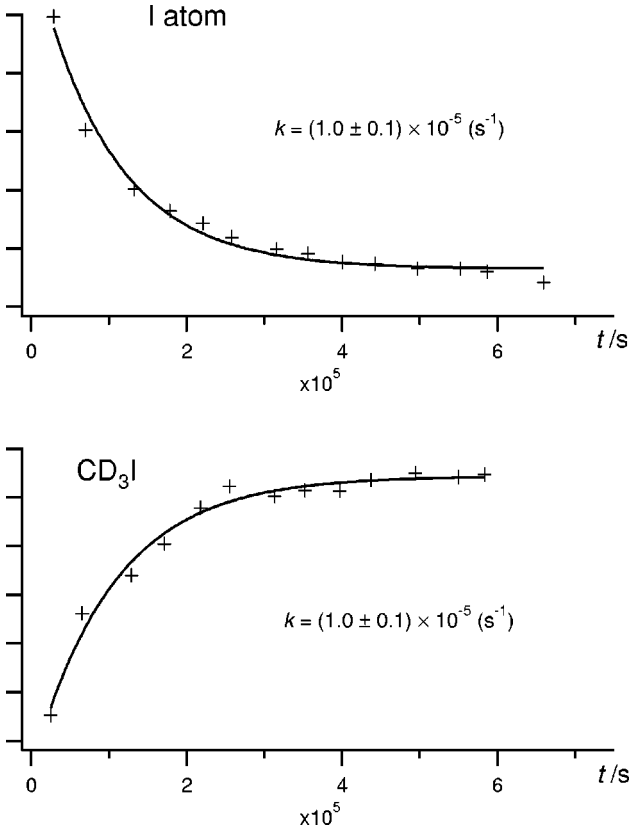

FIG. 7. The temporal changes of the absorption of I atom (7638 cm^{-1}) and CD_3I (947.3 cm^{-1}) in solid p-H_2. The solid lines represent least-squares fitting of the observed relative intensities to a single exponential function. The determined rate k is shown in each panel.

the geminately produced radicals and iodine atoms close to each other and were subjected to the following recombination:

$$R+I\rightarrow RI$$

$$(R=CD_3,\ CD_2H,\ CDH_2,\ CH_3). \qquad (6)$$

While there is no information on the distance between the reacting partners in the reaction (6), they may well be close enough to recombine at the low temperature of 5 K. The radicals far apart from the iodine atom are considered to be subjected to the tunneling reaction with the surrounding hydrogen molecules, which will be discussed in the next section.

2. Reaction between methyl radical and surrounding hydrogen

As repeatedly stated, one of the salient features of the p-H_2 matrix is that it allows *in-situ* photolysis because of the negligibly small cage effect.[35,36] In the present systems too the major process must be the photolytic separation of the pair of the radicals and the counterpart iodine atom. The subsequent major process is obviously the tunneling reaction between the radicals and the surrounding hydrogen molecules in the reaction (3).

Although the reaction (3) is a bimolecular reaction, the reaction in the present system should be treated as those of a unimolecular reaction, because the reaction rate in the

TABLE III. First-order rate constants for the increase in the intensity of the three methanes shown graphically in Figs. 5 and 6. The numbers in the table represent the first-order rate constant (k) in units of 10^{-6} s^{-1}. The second through sixth rows correspond to the three sets of conditions used in the experiments (see text in Sec. II).

	CD_3	CD_2H	CDH_2
No IR filter	3.24(5)	1.34(3)	0.97(4)
Filter (2170–3905 cm^{-1})	3.47(3)	2.00(2)	
Filter (1330–2240 cm^{-1})			0.95(4)
Filter (785–1390 cm^{-1})	3.46(4)		
Dark	3.0(1)		

present system does not depend on the concentration of H_2; all the radicals were surrounded by 12 H_2 molecules with the equal distance of ~3.8 Å at all times. Therefore, the number of methanes at time t, that is $N_{\text{methane}}(t)$, must be described by the following equation, where $N_{\text{methane}}(\infty)$ stands for the number at an infinitely long period:

$$N_{\text{methane}}(t)=N_{\text{methane}}(\infty)[1-\exp(-kt)]. \tag{7}$$

It could be said that the concentration dependence of H_2 molecules on the rate of the standard bimolecular reaction (3) is renormalized in the ''pseudo''-first-order rate constant k in Eq. (7). However, the crucial difference between standard ''gas phase'' bimolecular reactions and the reaction in the present system is that the interaction time between the radical and H_2 for the reaction is infinitely long in the present system, while it is very short in standard (high-temperature) gas phase reactions. The longer interaction time is characteristic of reactions at very low temperatures.[37] The first-order rate constants k determined by the least-squares fitting of the increase of the intensity of methane to Eq. (7) for each system are listed in Table III.

The rate constant k can be determined independently from the slowly decaying components of the radical. The decay of the number of the radical at time t, that is $N_{\text{radical}}(t)$, should be described by the following equation:

$$N_{\text{radical}}(t)=N_{\text{radical}}(0)\exp(-kt), \tag{8}$$

where $N_{\text{radical}}(0)$ stands for the number of radicals at $t=0$. Note that $N_{\text{radical}}(0)=N_{\text{methane}}(\infty)$, if the reverse of the reaction (3) is negligible. The rates k determined from the fitting of the slowly decaying components of the radical to Eq. (8) were comparable with those determined from the increase of the intensity of methane within the standard deviations. Since the intensity of the radicals consists of both rapidly and slowly decaying components, the uncertainty of the rate of the decay of the radical is larger than that of the increase of methane. Thus, we adopted the values determined by Eq. (7) for the following analysis of the reaction (3).

As the second row of Table III shows, the rate constant obtained by monitoring the absorption spectra without using any IR filter diminished as the degree of the deuteration in the radicals decreases. This tendency of the decrease in the rate constant with the decrease of the degree of the deuteration was also noticed in the experiments using the IR filters as is seen in the third through fifth rows of Table III.

As for the CD_3I system, we also tried to see any possible effect of the week-long IR beam which might affect the reaction through the excitation of the reactions to their vibrational excited states by using different filters or the measurement (3) stated in Sec. II. Temporal changes of the intensity of CD_3 and CD_3H are drawn in Fig. 5 for different conditions used in the experiments. It turned out that the effects of the IR light source on the rate constant of CD_3 were roughly within 10% as is seen in Table III.

D. Discussion

First, we discuss the effect of the monitoring IR beam of the spectrometer on the reaction rate. A disadvantage of using an FTIR spectrometer for the observation of the tunneling reaction is that the sample is exposed to the light source of the spectrometer during scans. Since the tunneling rate must depend on the quantum number of the vibration–rotation states of reactants, excitation by the light source, although very weak, may change the overall reaction rate. Fortunately, as shown in Table III, the effect of the light source on the rate of the CD_3 and CDH_2 systems was found to be negligibly small. Thus, the average of the rates shown in Table III can be considered to be the tunneling rate constant of the ground vibrational state of CD_3 and CDH_2, namely, $(3.3\pm0.3)\times10^{-6}$ s^{-1} for the system of CD_3 and $(0.96\pm0.05)\times10^{-6}$ s^{-1} for the system of CDH_2. Note that the tunneling rate of CD_3 determined here (3.3×10^{-6} s^{-1}) is slightly smaller than that we determined in the previous paper (4.7×10^{-6} s^{-1}).[9] The reason for the difference was that the rate we determined in the previous paper was actually the convolution of the tunneling process and the fast decay process due to the geminate recombination in the reaction (6) that we could not resolve in the previous work.

On the other hand, a significant increase in the tunneling rate of CD_2H was observed when the IR beam was filtered out except for the region of 2170–3905 cm^{-1} as shown in Table III. The increase of the tunneling rate of CD_2H with the IR filter may indicate that the tunneling rate of the backward reaction,

$$CD_2H+H_2\leftarrow CD_2H_2+H, \tag{9}$$

is accelerated by the excitation of the IR light of 3900–7500 cm^{-1}. However, it remains totally unexplained at the moment. The problem awaits further studies. In any case, it is safe to assume that the tunneling rate constant of the ground vibrational state of CD_2H is 2.0×10^{-6} s^{-1}.

As for CH_3, we did not observe any appreciable change of the spectrum of CH_3 nor CH_4 even one week after the radical was produced except for the fast decay component of the radical attributable to the geminate recombination reaction in the reaction (6). Since the sensitivity of our measurements was better than a few percent in absorption, we concluded that the change of the signal was at most 5% after one week. The reaction rate that yields a 5% signal change is calculated to be 8×10^{-8} s^{-1}. This must be the upper limit of the tunneling rate constant of the system of CH_3.

One of the important findings of the present study is that the tunneling rate depends drastically on the degree of deuteration of the radicals. In our previous paper the difference

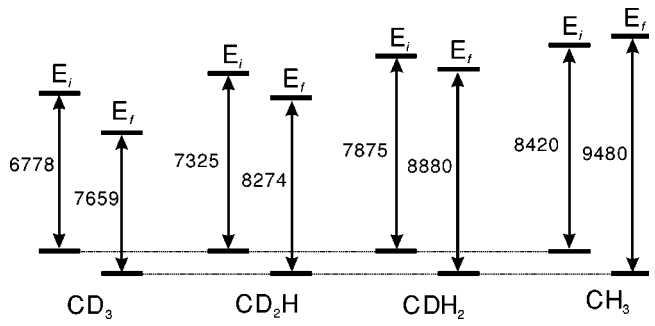

FIG. 8. The thermicities of $R+H_2 \rightarrow RH+H$ for $R=CD_3$ through CH_3. In each system, the left bars show energies of the reactant with (top) and without (bottom) the zero-point vibrational energies, and the right bars show those of the product. The numbers for the vertical lines represent the sum of the zero-point vibrational energies of the reactants (initial) and products (final). The units are in cm^{-1}. In order to make the values consistent, calculated vibrational frequencies were used for all the methyl radicals (Ref. 33), while vibrational frequencies observed in the gas phase were used for all the methane molecules (Ref. 31) and the hydrogen molecule (Ref. 29). The differences $\delta E = E_f - E_i$ are 881, 949, 1005, and 1060 cm^{-1} for the CD_3, CD_2H, CDH_2, and CH_3 systems, respectively. The horizontal bars at the bottom common to the four systems represent the energy levels of the potential minima for the initial (reactants) and the final (products) states. The upper horizontal bars show the levels with the zero-point energies included. The figure is drawn such that the final state with the zero-point energies (upper horizontal bar) is higher than the initial state for the CH_3 system, while the final states are lower than the initial states for all other systems.

in the reactivity between CD_3 and CH_3 in the reaction (3) was ascribed to the difference in the enthalpy including the zero-point energies of the reactants and products.[9] A similar discussion may be applied to all the deuterated systems. Figure 8 demonstrates the thermicity including the zero-point vibration energies for all the four isotopomeric systems. It is seen that as methyl radicals become heavier, the value of $\delta E = E_f - E_i$ decreases. Thus, if the criterion of the occurrence of the reaction depends upon *exo*- or *endo*-thermicity of the reaction as tentatively suggested in the previous paper, the demarcation line to divide the occurrence and nonoccurrence of the reaction seems to be between CDH_2 and CH_3 (see the upper horizontal bars in Fig. 8). However, such a discussion could be too crude as we only determined the upper limit of the reaction rate of the system of CH_3.

The tunneling reaction rate should be analyzed on the basis of the transition probability between the initial and final states of the reaction. An accidental degeneracy of the energies of the initial and final rovibrational states may drastically change the tunneling rate, which is known as the resonance effect.[37] Since the energy levels of the final (product) state are more dense for heavier systems due to the smaller rotational constant, the chance that the initial and final states resonantly overlap becomes larger for heavier systems, which may have relevance to the difference in the rate constants summarized in Table III.

Meanwhile, the difference in the potential energy surface of the whole reaction path should not be disregarded. The potential energy surface of the whole reaction path is slightly different for different degrees of deuteration due to the difference in zero-point vibrations.[28] The tunneling rate must be sensitive to such small differences in the potential energy surfaces. Precise calculation of the potential energy surface is necessary for further discussion.

IV. CONCLUSION

The significant conclusions of the present work can be summarized as follows:

(1) All the deuterated methyl radicals reacted with p-H_2 molecules at 5 K by tunneling to produce methanes. The first order rate constants of the tunneling reaction were determined to be 3.3×10^{-6} s^{-1}, 2.0×10^{-6} s^{-1}, and 1.0×10^{-6} s^{-1} for the CD_3, CD_2H, CDH_2 radicals, respectively. Conversely, the tunneling reaction between a CH_3 radical and the hydrogen molecule did not proceed within a week's time. The upper limit of the rate constant of the tunneling reaction CH_3+H_2 was estimated to be 8×10^{-8} s^{-1}.
(2) The effect of the monitoring IR beam upon the above reaction was not significant except for CD_2H.
(3) Most of the radical and its companion iodine atom were far separated upon the UV photolysis in solid p-H_2. However, some of the geminate pairs lie close enough to be subject to a rapid recombination to the parent iodide. The first order rate constant of 5×10^{-5} s^{-1} was about one order of magnitude larger than the other reaction involving the surrounding hydrogen molecule.

For deeper understanding of the tunneling effect on chemical reactions, further experimental studies are indispensable. Detailed experiments on the frequency dependence of excitation light on the tunneling rate will be necessary to clarify the quantum level dependence of the tunneling reaction. On the other hand, temperature dependence on the tunneling rate has not yet been studied yet, but it should be. This dependence will give us important information on the effect of the fluctuation of environments on the tunneling process. Solid parahydrogen will provide a useful matrix for such studies.

ACKNOWLEDGMENTS

This study was partially supported by Grant-in-Aid for Scientific Research of the Ministry of Education, Science, Culture, and Sports of Japan. The authors would like to thank Professor T. Ichikawa at Hokkaido University, Japan, for providing them the partially deuterated iodides.

[1] E. Herbst, Annu. Rev. Phys. Chem. **46**, 27 (1995).
[2] K. Toriyama, K. Nunome, and M. Iwasaki, J. Am. Chem. Soc. **99**, 5823 (1977).
[3] S. L. Baughcum, R. W. Duerst, W. F. Rowe, Z. Smith, and E. B. Wilson, J. Am. Chem. Soc. **103**, 6296 (1981).
[4] M. Petterson, E. M. S. Maçôas, L. Khriachtchev, J. Lundell, R. Fausto, and M. Räsänen, J. Chem. Phys. **117**, 9095 (2002).
[5] E. D. Sprague and F. Williams, J. Am. Chem. Soc. **93**, 787 (1971).
[6] A. Campion and F. Williams, J. Am. Chem. Soc. **94**, 7633 (1972).
[7] T. Miyazaki, K-P. Lee, K. Fueki, and A. Takeuchi, J. Phys. Chem. **88**, 4959 (1984).
[8] T. Kumada, K. Komaguchi, Y. Aratono, and T. Miyazaki, Chem. Phys. Lett. **261**, 463 (1996).
[9] T. Momose, H. Hoshina, N. Sogoshi, H. Katsuki, T. Wakabayashi, and T. Shida, J. Chem. Phys. **108**, 7334 (1998).
[10] T. Momose and T. Shida, Bull. Chem. Soc. Jpn. **71**, 1 (1998).

[11] D. P. Weliky, K. E. Kerr, T. J. Byers, Y. Zhang, T. Momose, and T. Oka, J. Chem. Phys. **105**, 4461 (1996).
[12] T. Momose, T. Miki, T. Wakabayashi, T. Shida, M.-C. Chan, S. S. Lee, and T. Oka, J. Chem. Phys. **107**, 7707 (1997).
[13] T. Momose, H. Katsuki, H. Hoshina, N. Sogoshi, T. Wakabayashi, and T. Shida, J. Chem. Phys. **107**, 7717 (1997).
[14] T. Momose, M. Miki, M. Uchida, T. Shimizu, I. Yoshizawa, and T. Shida, J. Chem. Phys. **103**, 1400 (1995).
[15] S. Tam, M. E. Fajardo, H. Katsuki, H. Hoshina, T. Wakabayashi, and T. Momose, J. Chem. Phys. **111**, 4191 (1999).
[16] H. Hoshina, T. Wakabayashi, T. Momose, and T. Shida, J. Chem. Phys. **110**, 5728 (1999).
[17] H. Katsuki and T. Momose, Phys. Rev. Lett. **84**, 3286 (2000).
[18] H. Katsuki, T. Nakamura, and T. Momose, J. Chem. Phys. **116**, 8881 (2002).
[19] M. E. Fajardo and S. Tam, J. Chem. Phys. **108**, 4237 (1998).
[20] S. Tam and M. E. Fajardo, Rev. Sci. Instrum. **70**, 1926 (1999).
[21] M. E. Fajardo and S. Tam, J. Chem. Phys. **115**, 6807 (2001).
[22] D. T. Anderson, R. J. Hnde, S. Tam, and M. E. Fajardo, J. Chem. Phys. **116**, 594 (2002).
[23] X. Wang, L. Andrews, S. Tam, M. E. DeRose, and M. E. Fajardo, J. Am. Chem. Soc. **125**, 9218 (2003).
[24] M. Fushitani, N. Sogoshi, T. Wakabayashi, T. Momose, and T. Shida, J. Chem. Phys. **109**, 6346 (1998).
[25] M. Fushitani and T. Momose, J. Chem. Phys. **116**, 10739 (2002).
[26] M. Fushitani, T. Momose, and T. Shida, Chem. Phys. Lett. **356**, 375 (2002).
[27] K. Kraka, J. Gauss, and D. Cremer, J. Chem. Phys. **99**, 5306 (1993), and references cited therein.
[28] Y. Kurosaki and T. Takayanagi, J. Chem. Phys. **110**, 10830 (1999).
[29] K. P. Huber, and G. Herzberg, *Molecular Spectra and Molecular Structure IV, Constants of Diatomic Molecules* (Van Nostrand, New York, 1979).
[30] G. Herzberg, *Molecular Spectra and Molecular Structure III, Electronic Spectra and Electronic Structure of Polyatomic Molecules* (Krieger, Florida, 1991).
[31] T. Shimanouchi, ''Molecular vibrational frequencies,'' in *NIST Chemistry WebBook, NIST Standard Reference Database Number 69*, edited by P. J. Linstrom and W. G. Mallard (National Institute of Standards and Technology, Gaithersburg, MD, 2003) (http://webbook.nist.gov).
[32] J. R. Riter, Jr. and D. F. Eggers, Jr., J. Chem. Phys. **44**, 745 (1966).
[33] J. L. Brum, R. D. Johnson III, and J. W. Hudgens, J. Chem. Phys. **98**, 3732 (1993).
[34] H. Hoshina, M. Fushitani, and T. Momose (unpublished).
[35] N. Sogoshi, T. Wakabayashi, T. Momose, and T. Shida, J. Phys. Chem. A **105**, 3077 (2001).
[36] T. Shida and T. Momose, in *Sciences of Free Radicals (in Japanese)*, edited by E. Hirota (Gakkai Shuppan Center, Tokyo, 1998).
[37] N. Balakrishnan and A. Dalgarno, Chem. Phys. Lett. **341**, 652 (2001).